JOURNAL OF AIRCRAFT
Vol. 47, No. 3, May–June 2010

Damage of Carbon/Epoxy Composite Plates Subjected to Mechanical Impact and Simulated Lightning

Paolo Feraboli* and Hirohide Kawakami†
University of Washington, Seattle, Washington 98195-2400

DOI: 10.2514/1.46486

Damage is inflicted on carbon-fiber/epoxy composite plates using both simulated lightning strike and mechanical impact in the effort to understand the relative effect of the two damage mechanisms. A methodology is proposed to characterize the damage resistance and tolerance of unconfigured composite plates subjected to lightning strike in a fashion that is consistent with the extensive work previously done on low-velocity impact. Using current and voltage diagnostics, it is possible to extrapolate the amount of electromechanical energy absorbed by the plate during the strike and compare it to that absorbed during a mechanical impact. Damage resistance is characterized by means of ultrasonic C-scans and microscopy, whereas residual strength is measured by means of compression after impact testing. Results show that the energy dissipated in a specimen during the lightning strike is much greater than the strain energy introduced by mechanical impact, and hence a comparison based on energy is not recommended. However, based on the relative threat levels associated with the impact and the lightning strike events, the comparison yields insightful observations on both damage state and residual performance. In general, for the configurations tested, lightning strike damage seems to be less detrimental than the mechanical impact in terms of both damage area and residual strength.

I. Introduction

A WIDE range of composite material forms are finding use in today's aerospace, automotive, and other transportation industry segments. These materials are finally fulfilling the promise of providing aircraft manufacturers with a cost-competitive alternative to aluminum alloys. The Boeing 787 Dreamliner, due to join the world's active fleet by mid-2009, features more than 50% carbon fiber reinforced polymers (CFRP) by structural weight [1]. Beside the direct benefits resulting from the greater specific mechanical properties, such as increased fuel efficiency and reduced pollutant and acoustic emissions, other indirect advantages of a CFRP-intensive airframe are reduced maintenance requirements and increased passenger comfort because of the superior fatigue- and corrosion-resistance characteristics of these materials. However, the introduction of composites in the primary structure of modern aircraft presents special problems with regards to the lighting strike threat. Although metallic structures, such as traditional aluminum airframes, are highly conductive, CFRP have a much lower electrical conductivity. Although carbon fibers are good conductors, the polymer matrix is an excellent dielectric and therefore reduces the overall conductivity of the composite laminate.

Lightning strike is a threat to all structures, whether metallic or composites, and requires careful consideration from a certification standpoint. Lightning can induce damage on a structure by melting or burning at lightning attachment points, resistive heating, magnetic force effects, acoustic shock, arcing and sparking at joints, and ignition of vapors in fuel tanks [2,3]. Of particular interest to CFRP or other conductive composites is damage resulting from acoustic shock and resistive heating. When lightning strikes, a large amount of energy is delivered very rapidly, causing the ionized channel to expand with supersonic speed. If the shock wave encounters a hard surface, its kinetic energy is transformed into a pressure rise, which causes fragmentation of the structure. On the other hand, resistive heating leads to temperatures rise, and in turn it initiates a breakdown of the resin/fiber interface by pyrolysis. If the gases developing from the burning resins are trapped in a substrate, explosive release may occur with subsequent damage to the structure.

Although extensive literature is available regarding the threat of foreign object impact damage to composites [4–6], limited work has been published to assess the structural performance of CFRP specimens following lightning strike damage [7,8]. In a previous study [8], the authors inflicted simulated lightning strike damage at three different current levels (10, 30, and 50 kA) on carbon/epoxy coupons in order to characterize their damage resistance and tolerance response. Both unnotched and filled-hole (using an aircraft-grade stainless steel Hi-Lok fastener) specimens were tested, all unpainted and unprotected. After damage was inflicted, the CFRP specimens were tested in tension and compression for residual strength. The residual tensile strength was in general mildly affected, both in the unnotched and filled-hole configurations, as well as the unnotched compressive strength. On the other hand, the filled-hole compressive strength was dramatically reduced, particularly for 30 and 50 kA strikes. The criticality of the compressive failure mode over the tensile is not surprising for composites, but the negative influence of the fastener is not intuitive. It was found that for unnotched specimens the damage tends to be confined to the outer plies in proximity of the strike location, whereas for filled-hole specimen, the damage tends to spread throughout the entire specimen thickness. The presence of the fastener has mixed effects: for low amperage strikes (10 kA), the fastener tends to absorb the majority of the damage; for higher amperages (30 and 50 kA), it acts as an amplifier by distributing the damage throughout the entire thickness of the specimen. It was observed that at the higher current levels, particularly for the filled-hole specimens, the size of the damage was too large for the small size of the specimens, which were rectangles of 12×1.5 in. (305×38 mm). As a result of this study, it was concluded that for future researcher it is recommended to use larger specimens, possibly square plates of at least 6×6 in. (127×127 mm). Furthermore, given the criticality of compression strength for filled-hole specimens, it was recommended to limit future research to this particular configuration.

The basic lightning protection regulation for airframes is the same for all vehicle categories and appears in the Federal Aviation Administration (FAA) Advisory Circular AC 25-21 [9] (Sec. 25.581),

Received 10 August 2009; revision received 17 October 2009; accepted for publication 12 November 2009.

*Assistant Professor and Director, Automobili Lamborghini Advanced Composite Structures Laboratory, Department of Aeronautics & Astronautics, Box 352400, Guggenheim Hall; feraboli@u.washington.edu (Corresponding Author).

†Graduate Research Assistant, Department of Aeronautics & Astronautics; Research Engineer, Japan Ministry of Defense, Tokyo.

Table 1 Threat levels associated with lightning strike and mechanical impact

Threat	Lightning strike, kA	Impact damage, ft · lb (J)
Very high	100–200	50–100 (67.8–135.6)
High	50–100	30–50 (40.7–67.8)
Medium	30–50	15–30 (20.3–40.7)
Low	0–30	0–15 (0–20.3)

which requires that the aircraft be able to sustain a lightning strike without experiencing catastrophic damage. These requirements are inherently nonspecific and allow manufacturers to adopt different certification strategies. However, SAE International provides aerospace recommended practices (ARP) that can be use to show compliance with these requirements [10,11]. The accuracy of the testing technique adopted as compared to real lightning strike events is fundamental question, and it has been discussed for decades. Previous work by NASA, FAA, and industry has led to the development of a recommended procedure: the SAE ARP 5412 [11], which is accepted internationally as the sole test standard by which to simulate lightning strike in a laboratory environment. The research presented here follows accurately the recommendations contained in [11].

Although regulatory agencies impose compliance with safety requirements, aircraft manufacturers also have internal requirements that address both safety and economic concerns. In a fashion similar to foreign object impact damage [4], whereby detection thresholds [such as barely visible impact damage] (BVID) and associated impact energy levels, are set to determine maintenance and inspection procedures, different threat scenarios exist for lightning strike damage. Table 1 summarizes the levels of threat for both impact and lightning strike damage that are of interest to airframe manufacturers. The peak impact energy levels and lightning strike currents employed are lower than the peak values presented in Table 1 because they are adjusted to be adequate for the dimensions of the specimens being considered. This study, although not focusing on the visual detectability aspects of the damage, aims at establishing a comparison between the relative severity of mechanical impact damage and lightning strike damage. The worst conditions for evaluating the residual strength in both types of damages are considered, which involve compressive loads. Also, the lightning strike specimens involve filled-hole configurations, which have been shown to cause greater damage than unnotched configurations [8].

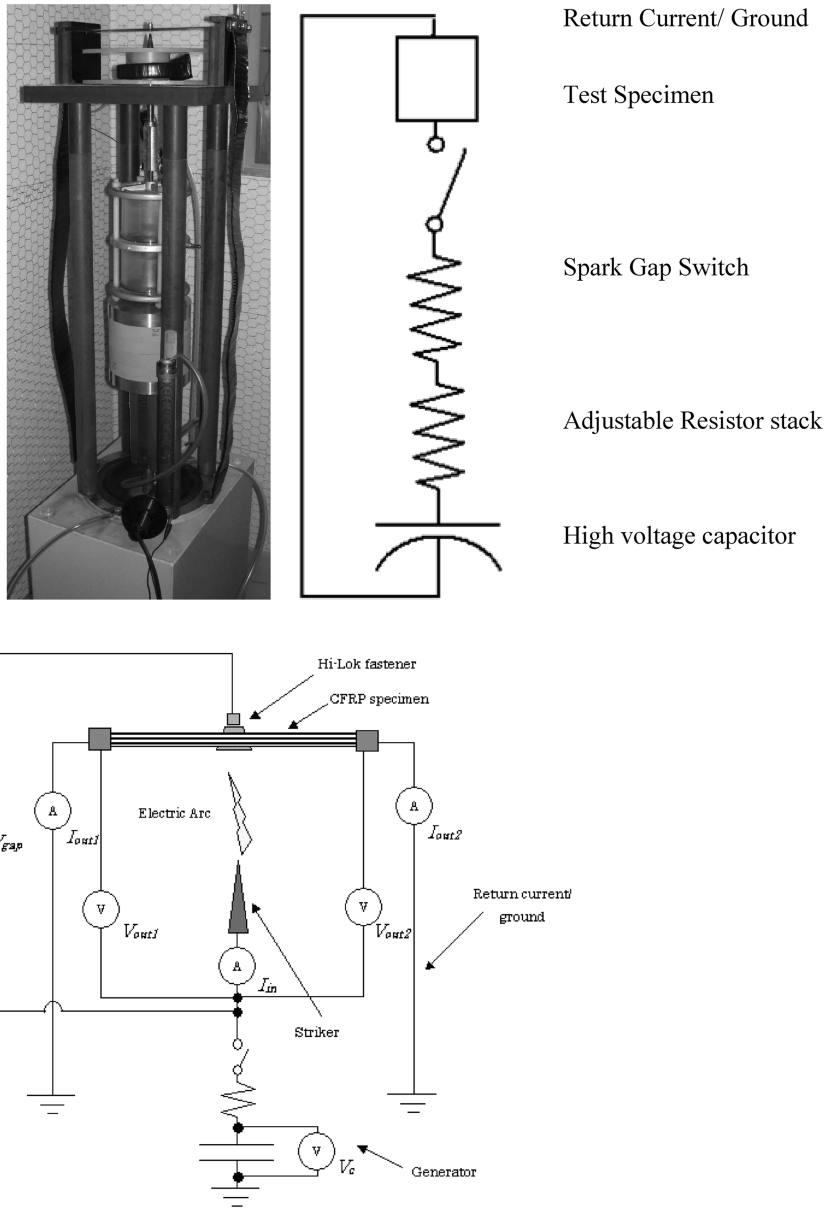

Fig. 1 Picture and schematics of the lightning strike generator.

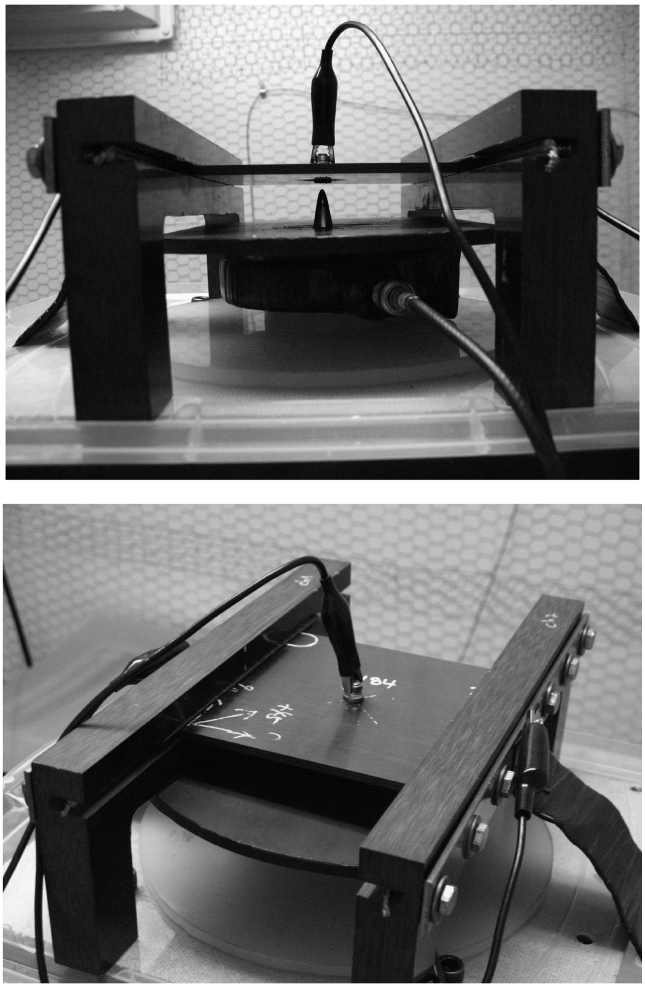

Fig. 2 Details of the test specimen area of the lightning strike generator.

II. Experimental Procedure

A. Description of the Lightning Strike Generator

The lightning strike generator developed at the University of Washington is composed of a high-voltage capacitor, a high-voltage resistor, an adjustable resistor stack, a spark gap switch, the test specimen, and the current return network, as shown in Fig. 1. The capacitor is capable of supplying 44 kV and 52 μF and the adjustable resistor stack is used to vary the amperage of the strike and to modulate the waveforms, while the spark gap switch is used to trigger the strike. The area in proximity of the test specimen is reported in more detail in Fig. 2 and shows the dielectric support frame, current and voltage probes, the conical copper striker, the CFRP coupon with the fastener, and the copper strips used to connect the specimen to the ground. The CFRP specimen is supported at the two short ends between two copper electrodes, for which the position is adjusted to be in close contact with the specimen and are encapsulated by nonconductive phenolic composites. Striker distance is kept constant for all tests at 0.125 in. (3.2 mm). The generator is contained in a chamber, which is electrically and physically separated from the surrounding environment in order to ensure safe operation. The lightning strike generator is capable of generating waveform D as specified in SAE ARP 5412 [11]. Waveform D is designed to represent a typical restrike after the primary strike to the airframe and is also used to certify the vast majority of the airframe acreage. Waveform D calls for a maximum of 100 kA, released over less than 0.5 μs [8].

Table 2 Voltage: current intensity and energy dissipated for the three threat levels of lightning strike used in this investigation

Threat	Capacitor voltage, kV	Resistance, Ω	Strike current, kA	Average energy dissipated in specimen, ft · lb (J)
High	29.1	0.3	70	720 (976)
Medium	30.3	0.6	50	572 (775)
Low	18.9	0.6	30	269 (364)

B. Lightning Strike Energy Calculations

According to the composite materials handbook-17 definition [12], damage resistance is a relationship between an external threat or event and the resulting state of damage in the structure. On the other hand, damage tolerance is defined as the relationship between the existing state of damage in the structure, independently of how it was introduced, and its residual performance. Although interconnected, these two properties are very distinct. Traditional damage resistance and tolerance studies [12,13] on composite materials investigate the relationship between the mechanical damage inflicted on a specimen, such as low-velocity impact [14] or quasi-static indentation [15] and the residual strength of the specimen [16]. These two relationships are often captured and summarized in two key plots [12,13] that show the relationship between projected damage area measured by ultrasonic C-scan and impact energy, and the relationship between residual strength as measured by compression after impact (CAI) and impact energy. Often, the residual strength is normalized against the pristine (or undamaged) value of the compressive strength. Although questions have been raised about the usefulness of the CAI test and its applicability to real configured structures for design and certification purposes, this systematic approach to impact damage characterization is well known to the composites community and, with its limitations, accepted by it. For lightning strike damage, a similar approach has not been use in the open literature, partly because of the experimental complexities associated with simulating lightning strike, and partly because lightning strike has been traditionally handled as an electrical and ignition related problem more so than a structural integrity threat. This study proposes a unifying methodology that can evaluate the relative threat of lightning strike damage to composite structures in a fashion similar to mechanical impact damage.

Energy is therefore the preferred metric by which mechanical impact threats are defined. For mechanical impact, the energy input into the specimen is dissipated in elastic deformation and vibration and damage creation. The elastic portion is returned to the rebounding impactor, whereas the remaining is dissipated and not returned to the specimen. For the majority of impact events used to inflict damage, the authors have shown that the energy returned is a small fraction of the total energy, although the bulk is dissipated in the formation of damage [4,5].

An electromagnetic threat, such as a lightning strike, releases large amounts of energy in the forms of thermal, electrical, and, to an extent, mechanical. However, for lightning strike, the severity of the threat is classified by the intensity of the current. The current that is generated by the capacitor and used to strike the specimen is always

Table 3 Summary of coupon level unnotched, open-hole, and filled-hole tests

Family	Repetitions	Hole diameter, in. (mm)	Length, in. (mm)	Width, in. (mm)	Nominal thickness, in. (mm)	Average gross strength, ksi (MPa)
Unnotched	3	——	12.0 (304.8)	1.5 (38.10)	0.180 (4.57)	101.9 (703)
Open hole	3	0.250 (6.35)	12.0 (304.8)	1.5 (38.10)	0.180 (4.57)	64.6 (445)
Filled hole	3	0.250 (6.35)	12.0 (304.8)	1.5 (38.10)	0.180 (4.57)	91.9 (634)

conserved. Although it is responsible for the creation of damage, its measure does not give any indication with regards to the extent of damage. On the other hand, voltage is not conserved, and its drop across the specimen can be used to calculate the energy dissipated during the event. To calculate the energy dissipated, it is necessary to devise a complex experimental setup that measures the voltage drop and the energy flow across the specimen during the strike. From the schematic of Fig. 1, it can be seen that the capacitor is charged by the user to the desired voltage V_c, at which point the switch in the spark gap is closed and the desired current I_{in} is introduced into the specimen. To have an accurate measure of I_{in} rather than an estimated value that may not account for the losses incurring between the capacitor and the striker, a current probe is positioned right below the striker. The air, which is a dielectric, breaks down and an electrical arc sparks between the striker and the fastener in the specimen. On the opposite side of the strike, a high-voltage probe is connected to the fastener to measure the voltage V_{gap}, which together with I_{in} defines the entire electrical state of the specimen at the time of the strike. The current then travels along the specimen toward the edges clamped in the copper electrodes, thus dividing into I_{out1} and I_{out2}, which are measured using other two current probes. The two copper electrodes constitute the current return network. The ability to measure both of these return currents guarantees that the strike is balanced and that there is no bias toward one of the copper electrodes. Additional high-voltage probes are also connected to the each of the copper electrodes and measure the voltage drop across the specimen as defined by V_{out1} and V_{out2}. Thus the current and voltage state of the specimen after the strike is fully defined.

With these values, it is then possible to calculate the energy dissipated during the strike. The definitions of electric power P is

$$P = I \cdot V \tag{1}$$

where I is the current and V the voltage, and integrating the power over the duration of the event the energy generated is

$$E = \int P \cdot \mathrm{d}t \tag{2}$$

The difference in potential between the fastener and one end of the specimen is $V_{\text{out1}} - V_{\text{gap}}$; thus, the energy consumed in one-half of the specimen is

$$E_1 = \int [I_{\text{out1}} \cdot (V_{\text{out1}} - V_{\text{gap}})] \cdot \mathrm{d}t \tag{3}$$

Similar considerations can be made for the other side. The total energy dissipated in the specimen is given by $E_{\text{diss}} = E_1 + E_2$ and using the relationship $I_{\text{in}} = I_{\text{out1}} + I_{\text{out2}}$, it is possible to write

$$E_{\text{diss}} = \int [I_{\text{out1}} \cdot V_{\text{out1}} + I_{\text{out2}} \cdot V_{\text{out2}} - I_{\text{in}} \cdot V_{\text{gap}}] \cdot \mathrm{d}t \tag{4}$$

To determine the energy dissipated in the lightning strike event, it is therefore necessary to measure three current values and three voltage values.

To verify that the calculations are accurate, it should be reminded that the energy dissipated in the formation of the arc between the striker and the fastener is

$$E_{\text{arc}} = \int [I_{\text{in}} \cdot V_{\text{gap}}] \cdot \mathrm{d}t \tag{5}$$

and that the nominal energy generated by the capacitor is given by

$$E_{\text{gen}} = \frac{1}{2} \cdot C \cdot V^2 \tag{6}$$

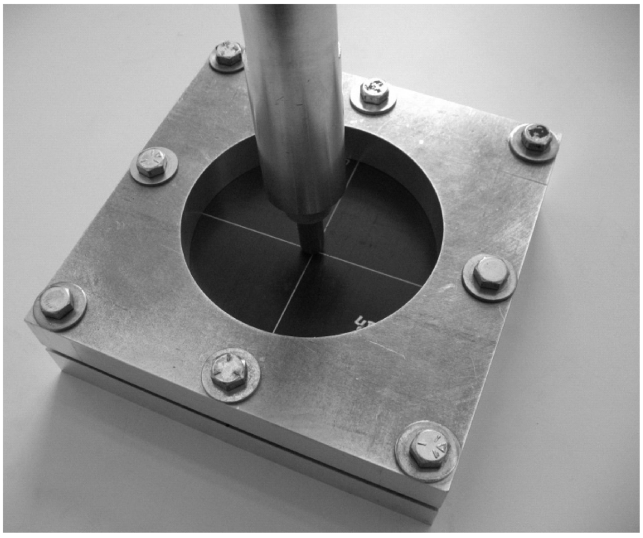

Fig. 3 Impact fixture and impactor.

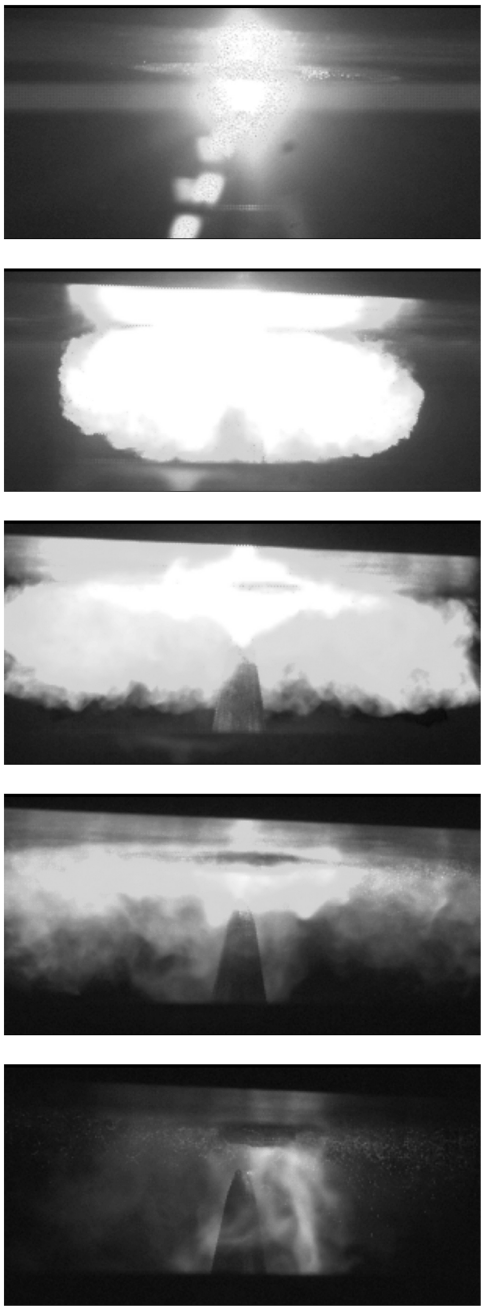

Fig. 4 Selected images extracted from a high-speed video recording of a 30 kA strike.

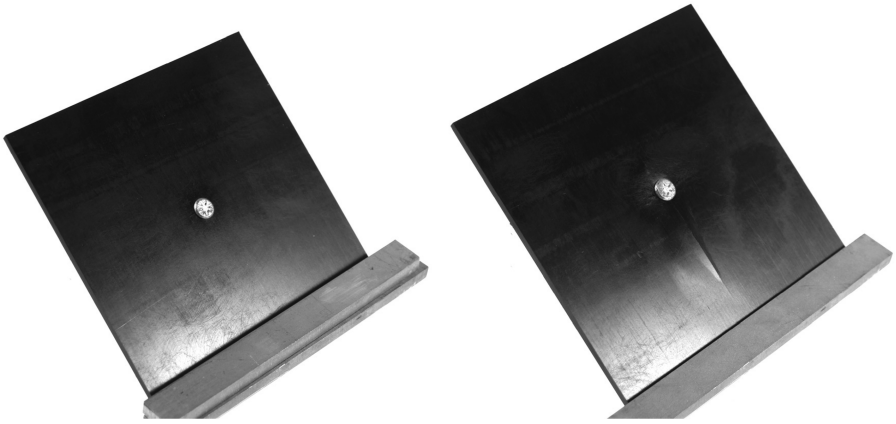

Fig. 5 Specimens with fastener following a 30 kA (left) and a 70 kA strike (right).

where C is the capacitance and V_c the voltage of the capacitor at the time of the strike.

For the conservation of energy,

$$E_{\text{gen}} = E_{\text{diss}} + E_{\text{arc}} + E_{\text{return}} \tag{7}$$

where E_{return} is the quantity remaining past the V_{out1} and V_{out2} measurements and that is either dissipated in the current return network or returned to the ground.

Table 2 shows the calculated energy dissipated into the specimen at the different current levels, corresponding to the threat levels of Table 1. It can be seen that for the equivalent threat level, the energy dissipated in a specimen subjected to mechanical impact is an order of magnitude lower than the energy associated to a lightning strike.

C. Specimen Fabrication and Test Setup

Flat panels, having dimensions 13×13 in. (330×330 mm) of Torayca T700S/2510 carbon-fiber/epoxy composites are fabricated

Fig. 6 Close-up of top and bottom surfaces of a filled-hole specimen subjected to a 50 kA strike.

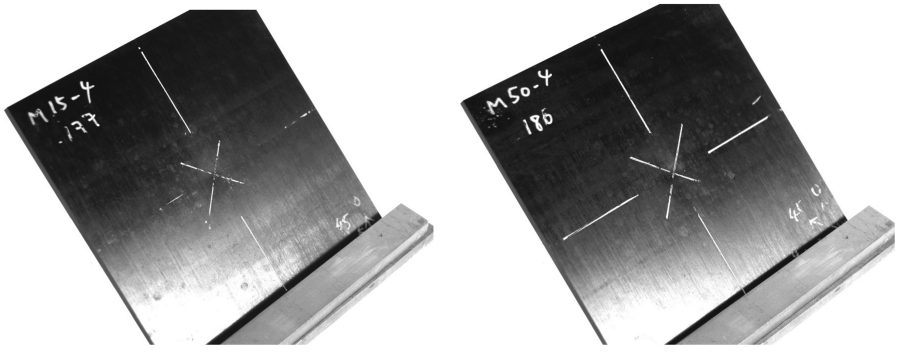

Fig. 7 Specimens following impacts at 15 ft · lb (20.34 J) (left) and a 25 ft · lb (33.89 J) (right).

Fig. 8 Ultrasonic C-scan of the postlightning strike specimens at 30, 50, and 70 kA.

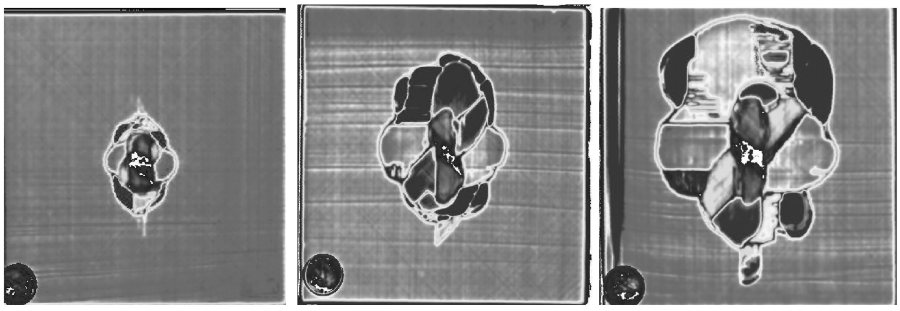

Fig. 9 Ultrasonic C-scan of the postimpact specimens at 5 ft · lb (6.78 J), 15 ft · lb (20.34 J), and 25 ft · lb (33.89 J).

by press molding for 60 min at 270°F (132°C) and 80 psi (0.55 MPa). This system is designated for primary structures of general aviation aircraft and was characterized during the FAA-sponsored Advanced General Aviation Technology Experiment program in the late 1990s and early 2000s. The layup is $[0_3/+45_2/0_4/-45_2/0_4/90_2]_S$, or (65/24/11), for a total of 34 plies and a nominal thickness of 0.180 in. (4.6 mm). After molding, test coupons are machined with a diamond-coated water-spray disk saw to the final dimensions of 6.0 × 6.0 in. (152 × 152 mm). The specimen dimensions for this study are purposely selected to be large than the ones used in the previous study by the authors [8] and allow for the lightning strike damage to be fully contained within the boundaries of the specimen. The specimens are then subjected to lightning strike or mechanical impact.

For the laminate stacking sequence considered in this study, a series of coupon level tests are performed to measure the unnotched, open-hole, and filled-hole compressive strength of the laminate. Specimens of dimensions 12 × 1.5 in. (304.8 × 38.1 mm) are tested using the Boeing-derived open-hole compression fixture of ASTM D6484 [17]. For the material and stacking sequence selected, it is found that compressive strength is relatively insensitive to the presence of a filled hole but very sensitive to an open hole. Detailed results are reported in Table 3. These values are of little use for the damage resistance and tolerance investigation performed in this study and, by themselves, are not sufficient for a complete definition of the laminate strength properties. However, they are generated to ensure that the results that the CAI observations that follow for unnotched and filled-hole plates are consistent with the laminate compressive strength properties.

For mechanical impact, the plates are clamped between the upper and lower portions of the indentation fixture specified in [15], which has a 5.0 in. (127 mm) diameter circular opening (see Fig. 3). The plates are impacted with a falling weight of 10 lb (4.54 kg) from different heights to achieve the desired impact energy [4,5]. For mechanical impact, the maximum energy cutoff threshold for BVID has been traditionally considered 100 ft · lb (135.6 J). However, in this study, energy levels of 5, 15, and 25 ft · lb (6.8, 20.3, and 33.9 J, respectively) are used. The upper energy threshold is highly dependent on the thickness of the material, and for the thickness considered in this study, an energy value of 100 ft · lb (135.6 J) is excessive. Already at 25 ft · lb (24.9 J), the projected damage area approaches the boundaries of the fixture, at which point the CAI results cease to be meaningful. The impactor is a 1.0 in. (25.4 mm) diameter solid steel impactor.

For the lightning strike, the plates are first drilled to accommodate a 0.25 in. (6.35 mm) diameter aircraft-grade stainless steel Hi-Lok fastener. Only filled-hole plates are tested for lightning strike damage based on the observations made by the authors in [8], and summarized in the previous sections. From a practical perspective, because fasteners are always present on the skin of an aircraft, even a composite-intensive one such as the Boeing 787 [1], lightning is known to typically strike the metallic fastener rather than the unnotched skin. Therefore, evaluating the effect on filled-hole specimens has a dual significance of both representing the most stringent damage condition and the most realistic. Following the installation of the fastener, specimens are introduced in the test area of the lightning apparatus and supported on two edges against the copper electrodes. The panels are unpainted and unprotected: although not representative of a flight-ready composite airframe

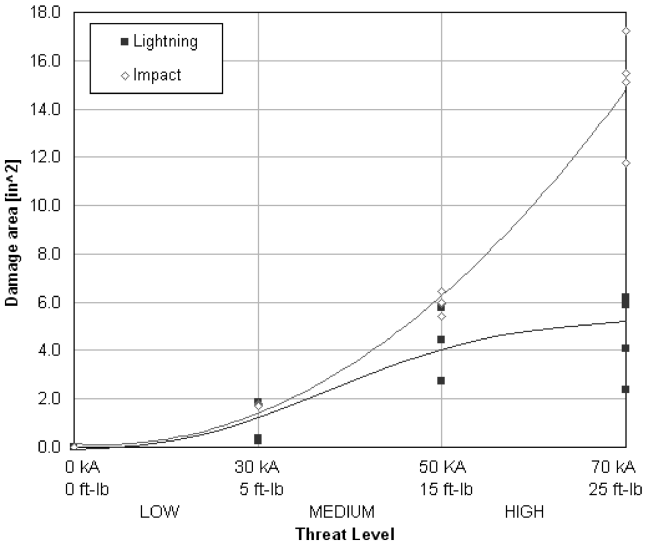

Fig. 10 Projected damage area for impact and lightning strike specimens.

Table 4 Summary of damage infliction tests

Family	Repetitions	Damage type	Threat	Fastener diameter, in. (mm)	Length, in. (mm)	Width, in. (mm)	Average damage area, in.^{2} (mm^2)
LF0	4	——	——	0.250 (6.35)	6.0 (152.4)	6.0 (152.4)	0.0
LF30	4	Lightning 30 kA	Low	0.250 (6.35)	6.0 (152.4)	6.0 (152.4)	0.60 (387)
LF50	4	Lightning 50 kA	Medium	0.250 (6.35)	6.0 (152.4)	6.0 (152.4)	4.42 (2852)
LF70	4	Lightning 70 kA	High	0.250 (6.35)	6.0 (152.4)	6.0 (152.4)	4.62 (2981)
M0	4	——	——	——	6.0 (152.4)	6.0 (152.4)	0.0
M5	4	Impact 5 ft · lb	Low	——	6.0 (152.4)	6.0 (152.4)	1.75 (1129)
M15	4	Impact 15 ft · lb	Medium	——	6.0 (152.4)	6.0 (152.4)	5.94 (3832)
M25	4	Impact 25 ft · lb	High	——	6.0 (152.4)	6.0 (152.4)	14.91 (9619)

structure, this configuration allows for focusing on the details of the CFRP material response to high electrical discharges alone. For this study, strikes at 30, 50, and 70 kA are used to inflict different states of damage to the coupons. All values are in line with the SAE recommended practice [11].

After introducing the impact or lightning strike damage, the specimens are removed from their respective fixtures and trimmed along the width to final dimensions of 6.0×4.0 in. (152×102 mm). They are subsequently clamped in the CAI fixture, according to ASTM International [17], and tested to failure to record the residual strength. As discussed in preceding sections, compression loads are known to be most critical for the residual strength assessment of CFRP panels following impact damage [12]. The authors have shown that filled-hole compression is also the most critical load scenario for CFRP specimens following lightning strike damage [8].

A total of 30 plate specimens are tested for residual strength, including unnotched pristine, unnotched postimpact, filled-hole pristine, and filled-hole postlightning strike. Tables 4 and 5 summarize the damage resistance and damage tolerance tests performed in this study. Nondestructive inspection is performed on 100% of the specimens via pulse-echo ultrasound using a C-scan system with a 5 MHz sensor. The projected damage area is then measured using image analysis software. Destructive inspection is performed by cross sectioning and optical microscopy of the lightning-damaged specimens. Two micrographic coupons are extracted from a single test specimen in order to reconstruct the damage state at the point of impact or strike in both the perpendicular and parallel to fibers direction. Mounting and sectioning lightning strike composite specimens is best accomplished with a two-stage mount [8]. The strike area of the specimen is first vacuum impregnated with the epoxy and then pressure cured to minimize formation of air bubbles. The encapsulated area preserves the fragile damaged material, as well as the fastener in place. Following the first mounting, the specimen is then sectioned and mounted a second time: this time for the polishing operation. The specimen is polished with a six-step process: 180 grit, 600 grit, 1200 grit, 9 μm, 3 μm silk, 3 μm nonnap polyester, and ending up with 1 h polishing with a nonnap polyester cloth and 10% alumina solution [8]. Rhodamine B laser dye is added to the mounting epoxy, which gives it a red–orange tint. The use of a laser-dyed backfilled epoxy is very important to distinguish between the composite's epoxy and the mounting epoxy. Without the dye, certain features can be subtle and contrast low, and they may go undetected.

III. Results and Discussion

A. Damage Infliction

Lightning strikes produce a loud sound, similar to that of a detonation, and generate a short, bright light, followed by a cloud of fire, smoke, and sparks because of the incandescent blast wave charged with carbon fiber particles and vaporized epoxy. Figure 4 is extracted from a high-speed digital video recording of the strike taken at 83,000 frames per second and using a set of polarized filters that reduce the intensity of the light.

For filled-hole specimens, the results vary between the low- and high-current strikes. In the majority of the strikes, the only damage visible is surface pitting of the fasteners on the head side, where the strike takes place (see Figs. 5 and 6). For this material system and stacking sequence, even at 70 kA, only minor bulging of the plies toward the surface is visible in the proximity of the fastener, and modest fiber breakage is observable on both top and backfaces. For mechanical impact, all specimens show a small dent on the side of the impactor, but even at the highest energy values, the dent does not become particularly deep nor leads to visible surface breakage (see Fig. 7).

Ultrasonic images for one representative filled-hole specimens at each of the three strike levels are reported in Fig. 8. In the pristine specimen, the fastener appears as a white round with an area of approximately 0.05 in.^{2} (32.2 mm^2). For the 30 kA, strike the damage area is contained in the fastener itself or in the immediate proximity of the fastener hole. For the 50 and 70 kA strikes, however, there appears to be a radical increase in damage area, and a large portion of the specimen appears damaged. The projected damage area is highly oriented along the direction of the zero axis, which corresponds to the direction along which the panel is clamped in the copper electrodes.

For mechanical impact, ultrasonic images reveal that already at 5 ft · lb (6.8 J), the state of internal damage is quite large, and at 25 ft · lb (33.9 J), it has almost reached the boundaries of the test fixture (see Fig. 9). In general, the projected area of the impact damage is more circular compared to the highly elliptical one of the lightning strike.

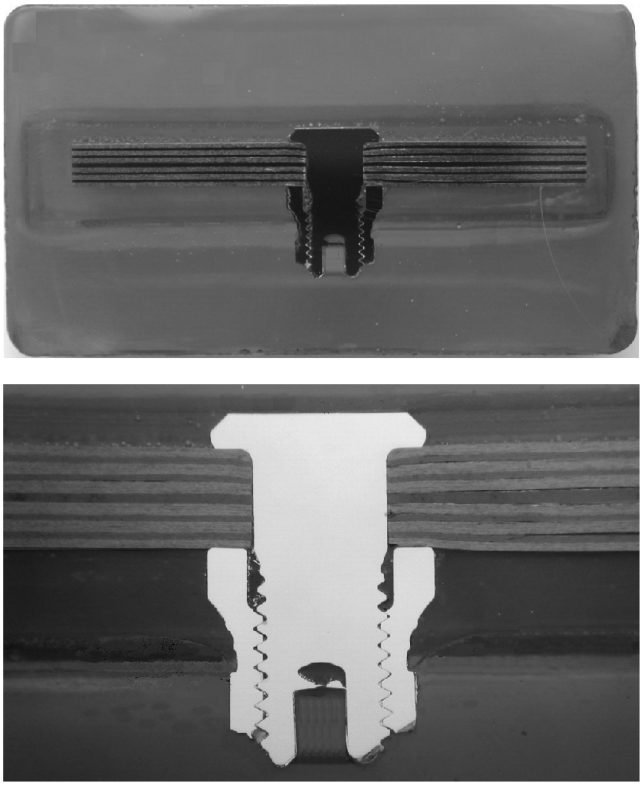

Fig. 11 Mounted and polished filled-hole specimen after lightning strike.

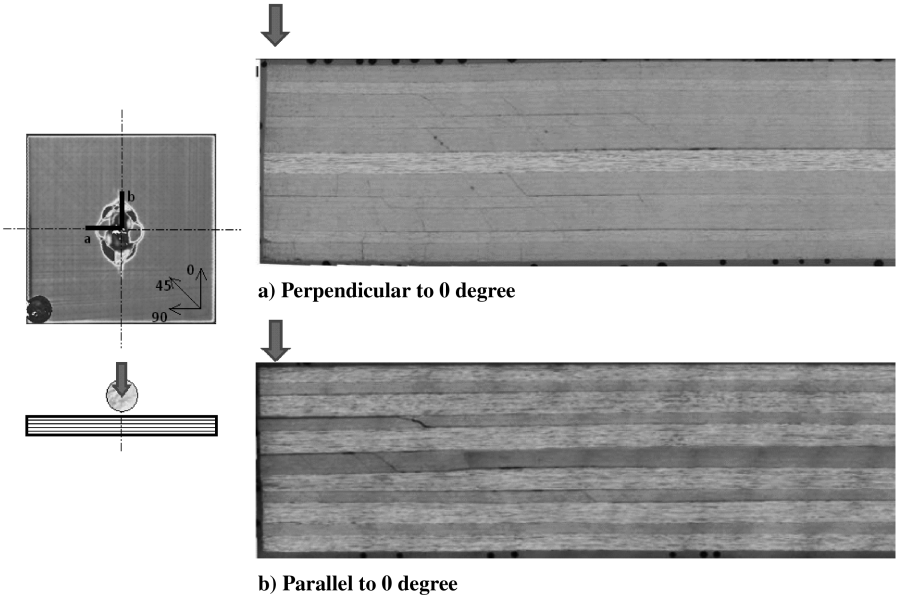

Fig. 12 Micrographic images at 50 times magnification in the directions parallel and perpendicular to the 0 deg axis for a 5 ft · lb (6.78 J) impact specimen.

Trends in projected damage area observed for filled-hole specimens subjected to lightning strike and for unnotched specimens subjected to impact damage are reported in Fig. 10. The plot shows projected damage area against severity of threat level, as described in Table 1. Results are summarized in Table 4. In general, the damage because of mechanical impact is much greater than the one caused by lightning strike, and the variation in measured data is much lower. The variability associated to lightning strike damage of filled-hole CFRP specimens is due to the relative fit of the fastener in the plate. Although not easily quantifiable, the degree of fit of the fastener in the hole has a great effect on the resulting damage. If the gap between the fastener and the laminate is sufficiently large, the electrical path is interrupted, and arcing between the fastener and the neighboring plies occurs. This results in a larger damage area. For the lightning strike, it should be noted that between the 50 and the 70 kA strikes, the damage area reaches an asymptotic value. This phenomenon is not easily explained because the variation in results is so high, as discussed just previously. However, a possible explanation is that once the current reaches all plies along the thickness by passing through the fastener, the incremental amount of damage area is so widely distributed that the projected damage area does not increase significantly. It should also be noted that a similar phenomenon is expected to occur, for different reasons, for mechanical impact specimens as well. For values of impact energy higher than tested in this study, a plateau would be reached as the damage area approaches the size of the circular aperture (i.e., the unsupported area).

B. Micrographic Inspection

For all specimens, microscopy is performed perpendicular as well as parallel to the 0 deg fiber direction and at the midpoint of the impact/strike location (see Fig. 11). For both damage types and for all threat levels, specimens show extensive matrix damage in the form of intraply cracks and interply delaminations. Fiber breakage is very modest, if at all present. Detailed analysis of the microscopic damage is beyond the scope of this study and will be the subject of a separate publication. However, stereomicroscopy is used here to further assess the extent and location of the damage to complement the observations performed by visual and ultrasonic inspections.

The mechanisms associated with the onset and propagation of impact damage in composite are not well understood. Hertzian contact and flexural deformations are responsible for the complex multi-axial stress state at the point of impact and can, in part, justify the formation of the well-documented delamination trees following an impact event [12]. Yet, although years of research have been dedicated to characterizing impact damage on composites, it can be said with a certain degree of confidence that the mechanisms by which a delamination originates at a given point, progresses for a certain length, and then changes plane in the form of a transverse matrix crack are not clear. Furthermore, the influence of target characteristics, such as stacking sequence, on impact damage resistance and tolerance has been assessed in several research studies, but it cannot be claimed that a thorough understanding of the complex interactions that exist between neighboring plies has yet been achieved.

The specimens obtained from the plate impacted at 5 ft · lb (6.78 J) energy (see Fig. 12) show multiple 45 deg shear cracks emanating down into the laminate from the point of impact. These cracks run parallel to each other within a stack of plies of the same orientation, and then they propagate longitudinally along the next interface of plies in the form of delaminations and eventually shear through the

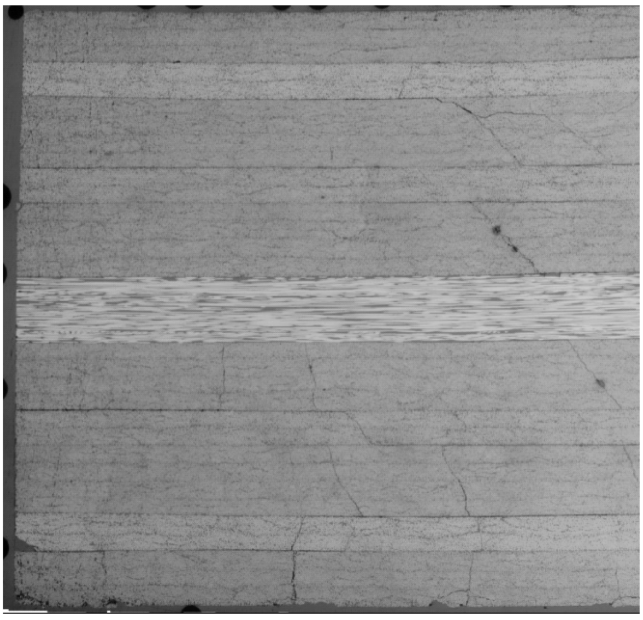

Fig. 13 Detail of the specimen impacted at 5 ft · lb (6.78 J) perpendicular to the 0 deg fibers and underneath the point of impact.

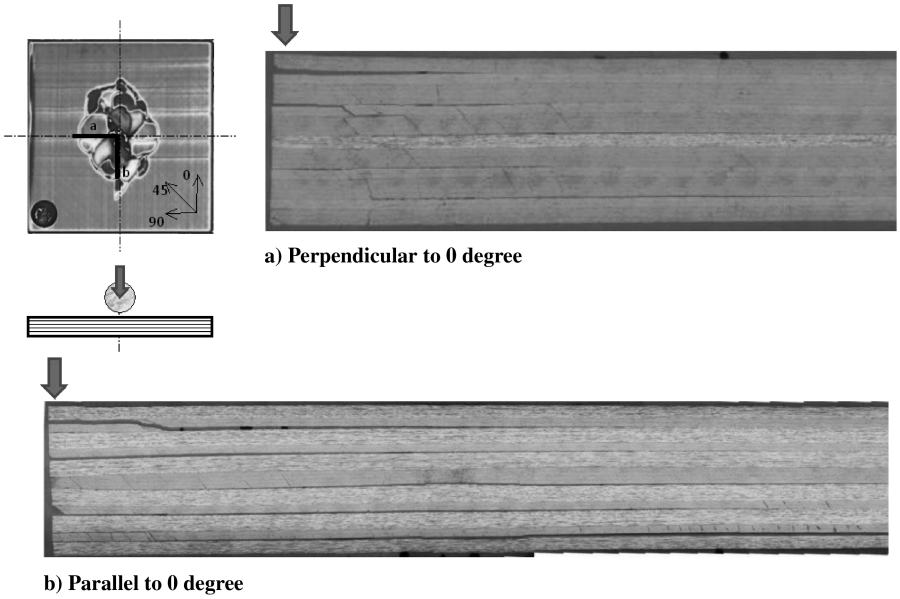

Fig. 14 Micrographic images at 50 time magnification in the directions parallel and perpendicular to the 0 deg axis for a 15 ft · lb (20.34 J) impact specimen.

next stack of plies (see Fig. 13). This is the typical aspect of a delamination tree and is characterized by few thin and short delaminations for the majority of the polished specimen. The area right underneath the impact point appears mostly pristine. Below the midplane of the laminate, there appears to be extensive cracking perpendicular to the plies, rather than at 45 deg, which suggest to be tensile matrix cracks in the 90 deg direction. At 15 ft · lb (20.34 J), the overall aspect of the cross section is the same (see Fig. 14), but the delaminations are larger and more diffused with complete separation of some of the ply stacks from the neighboring ones (see Fig. 15). There appears to be minor fiber breakage on the backface. For 25 ft · lb (33.89 J), the amount of damage in the upper portion of the laminate is very extensive with fiber breakage more diffused at the backface (see Figs. 16 and 17).

For lightning strike damage, the situation is even more complex, given the electromagneto–thermomechanical nature of the threat, and the amount of research performed in the open literature to this day is very limited. Lightning strike damage is a very complex phenomenon, which is possibly even more dependent on the characteristics of the target. Damage is thought to occur as a result of the fact that the electrical conductivity of the plies is not sufficient to conduct the electrical current associated with the lightning strike event. The resistive heating that results is sufficient to pyrolize the resin and generates cracks and burns in the matrix. Simultaneously, at the interface between neighboring plies, the mismatch in electrical conductivity can lead to mechanical separation in the form of delaminations. The electrical properties of composite materials have not been thoroughly studied as the mechanical ones. The literature to date does not offer suggestions in the electrical properties of multidirectional laminates, neither in the elastic region, which corresponds to the electrical response to currents that do not result in permanent damage, nor in the postelastic region, which corresponds to currents that result in the formation of damage. Nonetheless, stacking sequence is potentially even more influential for this type of threat than for mechanical impact, so the results obtained here pertain specifically to the laminate layup considered. Future research should be aimed at characterizing the damage mechanisms associated with electrical currents for basic unidirectional plies, as well as multidirectional laminates, and it is anticipated that it will result in a better understanding of the complex lightning strike phenomenon. This section is limited to describing and comparing the observations made on these specific specimens, which have been damaged by means on mechanical impact and lightning strike.

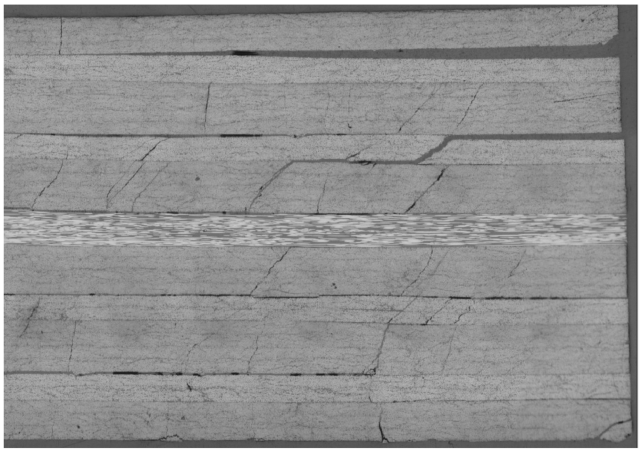

Fig. 15 Detail of the specimen impacted at 15 ft · lb (20.34 J) perpendicular to the 0 deg fibers and underneath the point of impact.

For specimens subjected to the 30 kA strike (see Fig. 18), damage is dispersed throughout the thickness of the laminate but is confined to a small region in the proximity of the fastener. This damage appears in the form of matrix cracks within the plies and delaminations at the ply interfaces. These cracks emanate from the fastener hole and propagate both downward and upward in the laminate, usually parallel or at a small angle from the longitudinal (see Fig. 19). The plies that appear most damaged are the offaxis plies, in particular the 45 deg stacks and the interfaces between the 45 and the 0 deg stacks. For 50 kA strikes, entire portions of the 45 and 90 deg stacks are separated, both in the through-the-thickness direction and longitudinally (see Fig. 20). Damage is very extensive, particularly in the section polished parallel to the fibers, which also corresponds to the portion of the C-scan with the highly elongated damage area. Long delaminations are visible in the laminate, particularly at the interface between zero-ply stacks and either ± 45 or 90 deg ply stacks. The 0 deg plies on the upper and lower surface are also highly damage right under the fastener head and collar with complete separation and vaporization of small chunks of material (see Fig. 21). At 70 kA, the 90 deg stack at the midplane in the region around the fastener is composed of a dense network of cracks and splits, which eventually lead to the formation of long delamination fronts (see Figs. 22 and 23). Partial fragmentation of the 0 deg ply stacks suggests that the fastener has the effect of distributing the electrical load to all the plies in its contact or proximity.

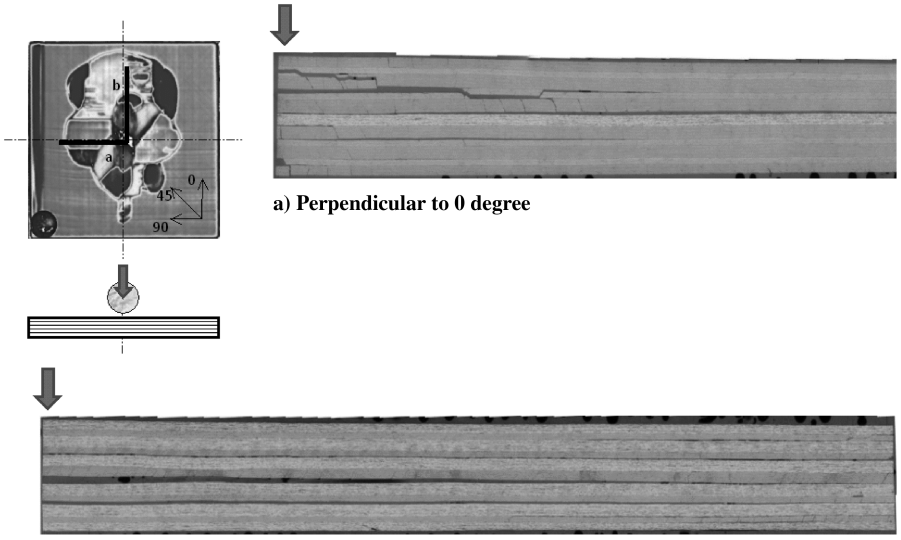

a) Perpendicular to 0 degree

b) Parallel to 0 degree

Fig. 16 Micrographic images at 50 times magnification in the directions parallel and perpendicular to the 0 deg axis for a 25 ft · lb (33.89 J) impact specimen.

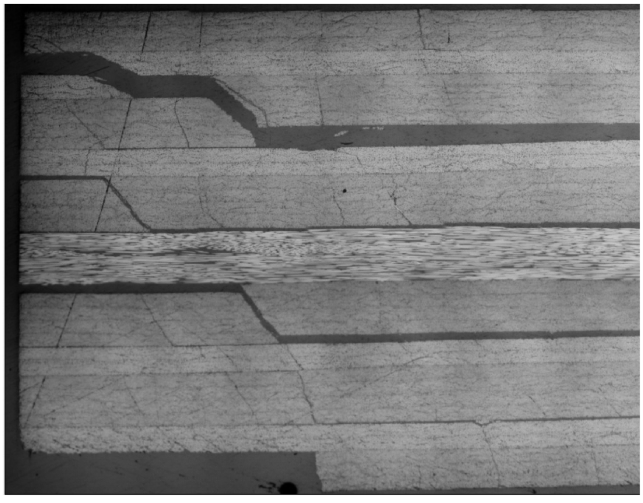

Fig. 17 Detail of the specimen impacted at 25 ft · lb (33.89 J) perpendicular to the 0 deg fibers and underneath the point of impact.

C. Residual Strength

After inflicting damage onto the specimens, these are tested to failure using the Boeing-derived CAI fixture [17] to quantify the loss in mechanical performance because of the presence of damage (see Fig. 24). For both pristine and filled-hole specimens, strength is calculated based on the gross section area, consistently with aerospace practice [12]. All specimens reported failed in the net section by an acceptable accepted compression failure mode as indicated by ASTM [17] (see Fig. 25).

Results for residual strength are reported in Table 5 and plotted in Fig. 26 against the severity of the threat and, in Fig. 27, against the projected damage area. This plot uses normalized strength values, which are obtained as the ratio of the damaged strength over the pristine or control strength. For impact damaged specimens, the normalized strength is calculated as

$$\sigma_{\text{NORM}} = \frac{\sigma_D^{\text{UN}}}{\sigma_0^{\text{UN}}} \tag{8}$$

where σ_0^{UN} is the pristine CAI strength of the unnotched plate and σ_D^{UN} is the damaged CAI strength of the unnotched plate. For lightning strike damage, the normalized strength is calculated as

$$\sigma_{\text{NORM}} = \frac{\sigma_D^{\text{FH}}}{\sigma_0^{\text{FH}}} \tag{9}$$

where σ_0^{FH} is the pristine CAI strength of the filled-hole plate and σ_D^{FH} is the damaged CAI strength of the filled-hole plate. For this material system and layup, the unnotched and filled-hole pristine CAI strengths are virtually identical (see Table 5), consistently with

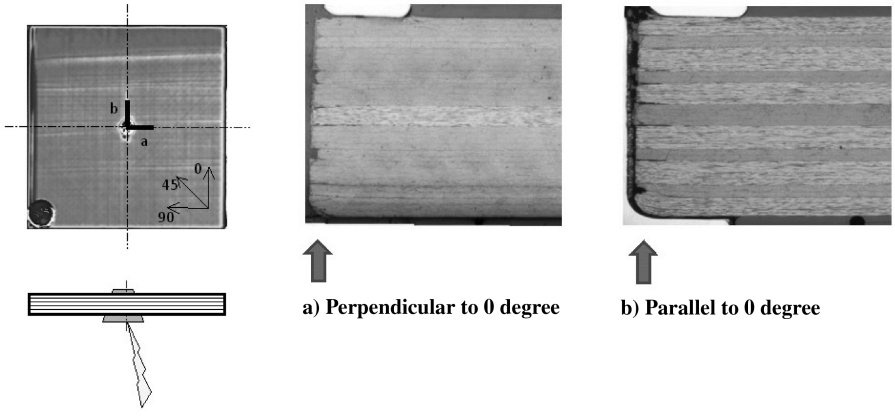

a) Perpendicular to 0 degree

b) Parallel to 0 degree

Fig. 18 Micrographic images at 50 times magnification in the directions parallel and perpendicular to the 0 deg axis for a 30 kA lightning strike specimen.

Fig. 19 Detail of the specimen struck with 30 kA, polished parallel to the 0 deg fibers in the proximity of the fastener collar.

the observations performed at the coupon level, as reported in Table 3.

In general, the residual strength following a mechanical impact is much lower than following a lightning strike of the same threat level. Mechanical impact appears to pose a more severe threat to this particular laminate material and layup, consistently with the greater area of damage reported in Fig. 10. The CAI strength following mechanical impact reaches a plateau between 40 and 50% of the pristine strength, and does not decrease further for increasing impact energy levels. For lightning strike damage, that is not the case, and the residual strength appears to continue to decrease for increasing threat levels and size of damage area.

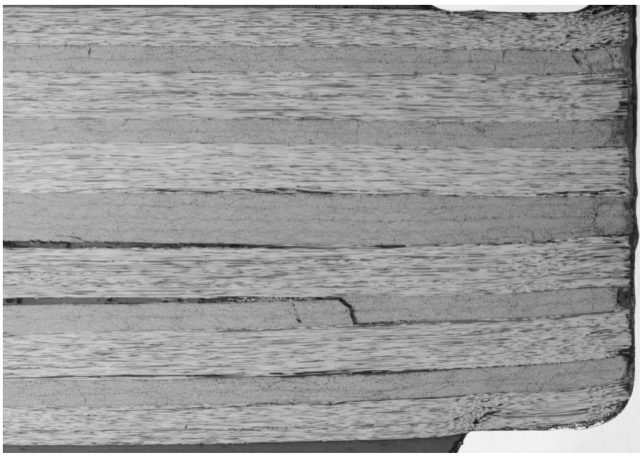

Fig. 21 Detail of the specimen struck with 50 kA, polished parallel to the 0 deg fibers in the proximity of the fastener head.

D. Discussion

This study suggests a procedure to evaluate the damage resistance and tolerance of carbon-fiber/epoxy composite panels subjected to lightning strike, which is a relatively novel area of research given the very limited amount of published work in the open literature. It uses an approach that has been recognized and accepted by the composites community for assessing the effect of impact damage and extends to the evaluation of lightning strike damage.

Considerations on the relative severity of impact damage and lightning strike damage are based on threat level rather than energy. The energy dissipated in a lightning strike event has been measured by means of current and voltage probes positioned strategically before and after the strike location. However, the amount of energy dissipated in the lightning strike event is an order of magnitude larger than the energy associated with an impact event of similar threat level. This makes the direct comparison of damage resistance and tolerance performance of the specimens subjected to impact and lightning strike threats difficult, as shown in Figs. 28 and 29. On the other hand, comparative evaluations can be performed successfully based on the relative severity of the threat level using impact energy and current intensity, respectively, as key threat metrics (see Figs. 10 and 26).

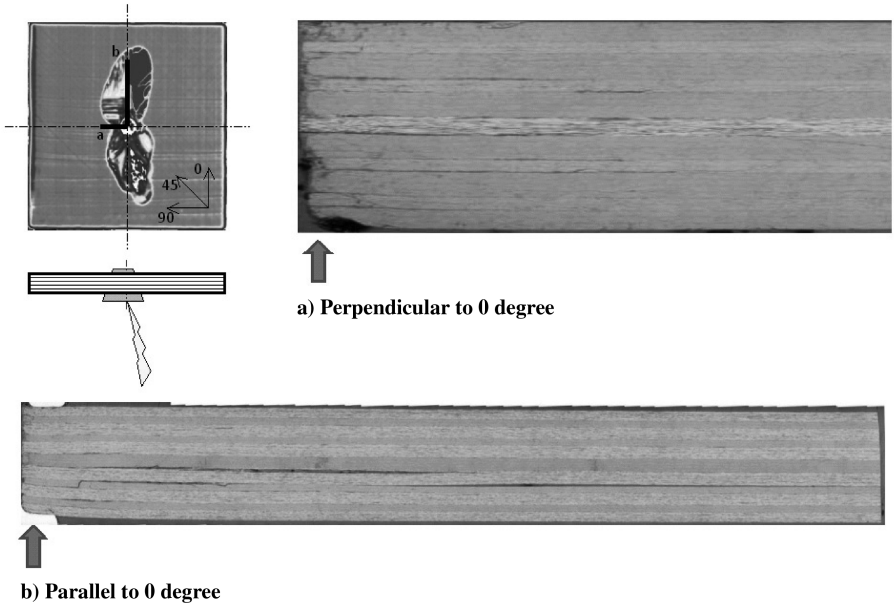

Fig. 20 Micrographic images at 50 times magnification in the directions parallel and perpendicular to the 0 deg axis for a 50 kA lightning strike specimen.

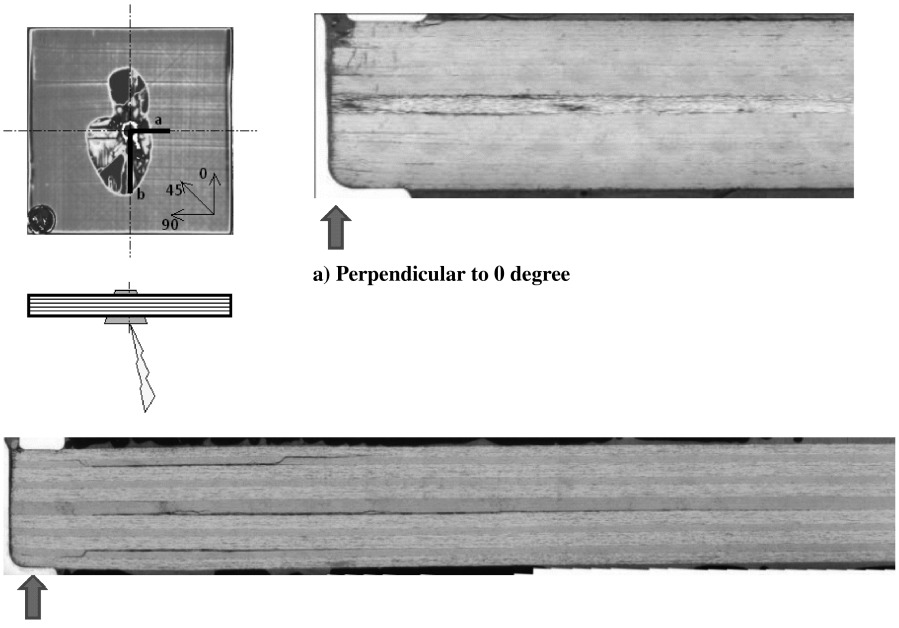

Fig. 22 Micrographic images at 50 times magnification in the directions parallel and perpendicular to the 0 deg axis for a 70 kA lightning strike specimen.

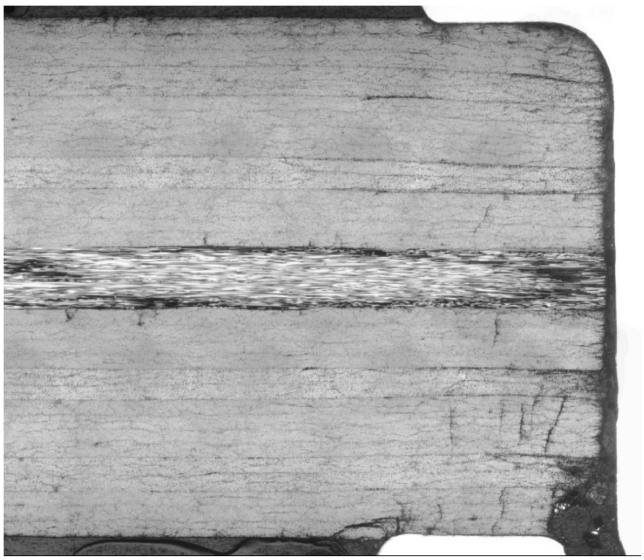

Fig. 23 Detail of the specimen struck with 70 kA, polished perpendicular to the 0 deg fibers in the proximity of the fastener head.

This study selected a specific composite target configuration to validate the use of this approach. From the results shown, it appears that impact damage is a greater threat to carbon/epoxy composite plates than lightning strike. However, it is important to remind the reader of the limited applicability of some of these results. First and foremost, these results apply only to the given prepreg tape material and hence cannot be extended to other material types. In particular, material properties, such as fiber architecture (fabric vs tape) and through-thickness conductivity (influenced by resin-rich interlaminar layers), are thought to be responsible for very different damage behavior under lightning strike and can lead to much greater damage states. Second, these observations are drawn on specimens that are unpainted. The presence of a relatively thick paint layer on a flight structure has negligible influence on its impact damage performance but is thought to be highly detrimental for lightning strike damage [2,3] because the paint is a good dielectric. Third, the specimens tested are all unprotected, which means they do not use any sort of lightning strike protection (e.g., a metallic wire mesh). This type of protection is known to be very effective in reducing the extent of lightning strike damage [2,3]. Fourth, the specimens tested for lightning strike damage are all filled hole. The presence of the steel fastener leads to more extensive damage than what is observed

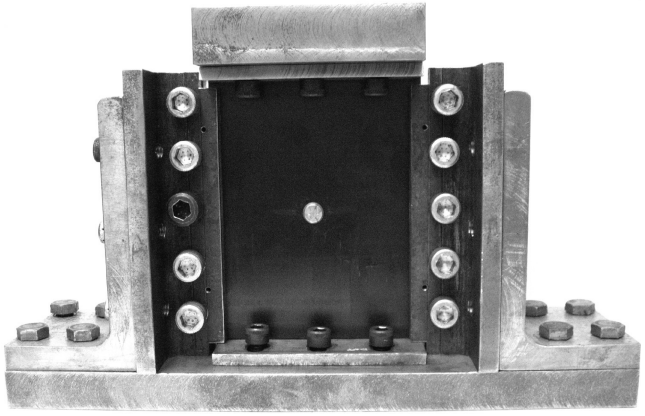

Fig. 24 CAI test fixture with filled-hole specimen following lightning strike damage.

Fig. 25 70 kA lightning strike specimen (left) and 25 ft · lb (33.89 J) impact specimen (right) following residual strength CAI testing.

Table 5 Summary of residual strength tests

Family	Repetitions	Threat	Residual strength test	Length, in. (mm)	Width, in. (mm)	Average residual strength, ksi
LF0	3	——	CAI	6.0 (152.4)	4.0 (101.6)	65.8 (454)
LF30	3	Low	CAI	6.0 (152.4)	4.0 (101.6)	62.7 (432)
LF50	3	Medium	CAI	6.0 (152.4)	4.0 (101.6)	58.0 (400)
LF70	3	High	CAI	6.0 (152.4)	4.0 (101.6)	44.5 (307)
M0	3	——	CAI	6.0 (152.4)	4.0 (101.6)	63.8 (440)
M5	3	Low	CAI	6.0 (152.4)	4.0 (101.6)	45.9 (316)
M15	3	Medium	CAI	6.0 (152.4)	4.0 (101.6)	28.3 (195)
M25	3	High	CAI	6.0 (152.4)	4.0 (101.6)	27.8 (192)

in identical but unnotched specimens [8] and diffuses it throughout the laminate thickness, thus making it the worst-case scenario. Fifth, these results are drawn on a specific laminate stacking sequence. Although stacking sequence has a large influence on the mechanical impact response of a plate, it has an even greater role on its lightning strike damage response. The relative orientation of the 0 deg fibers with respect to the current electrodes, as well as the orientation of the outer plies, can highly affect the overall state of damage in the laminate. If the same layup were to be tested in the lightning strike setup rotated by 90 deg, with the outer plies parallel to the copper electrodes rather than perpendicular, different results would be obtained. On the other hand, for impact damage, there would be no difference because both impactor and support fixture are axisymmetric. Evaluation of the influence of these parameters is beyond the scope of this study and shall be left for future research activities. Nonetheless, this paper defines a procedure that could be used successfully in those studies to assess the relative performance of carbon/epoxy specimens under impact and lightning strike threats.

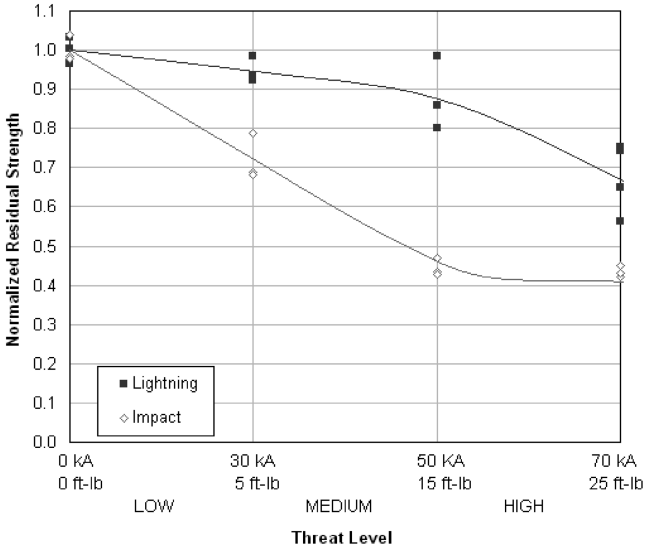

Fig. 26 Normalized CAI strength as a function of threat level for impact and lightning strike specimens.

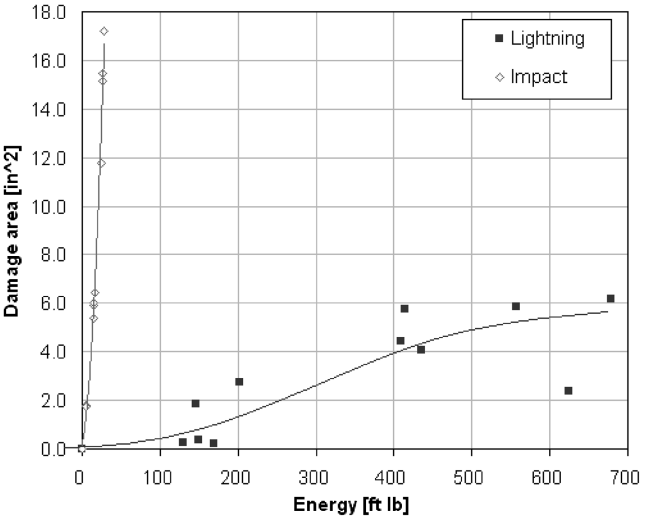

Fig. 28 Damage area for mechanical impact and lightning strike as a function of input energy.

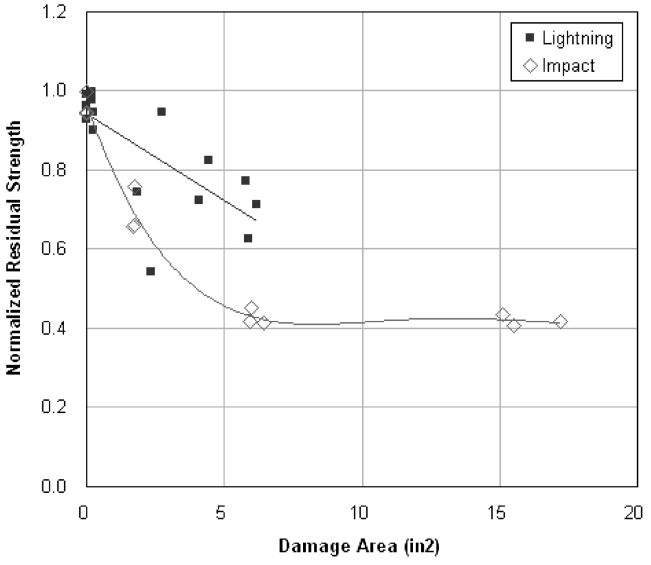

Fig. 27 Normalized CAI strength as a function of projected damage area for impact and lightning strike specimens.

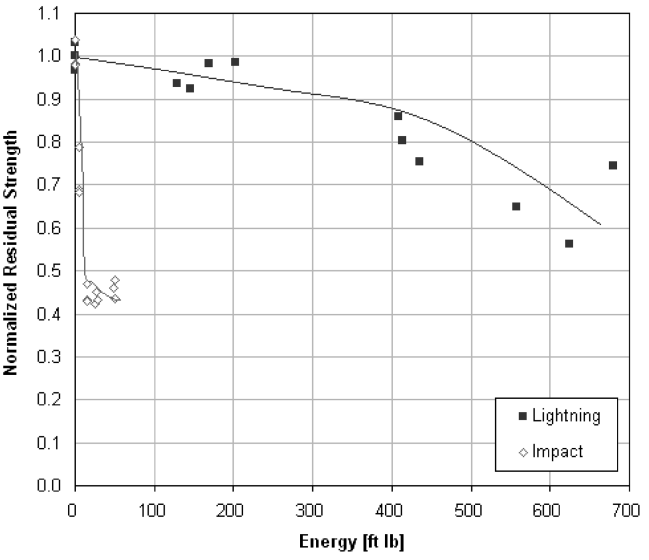

Fig. 29 Normalized CAI strength as a function of input energy for impact and lightning strike specimens.

IV. Conclusions

The study compares the relative severity of lightning strike damage and mechanical impact damage on the residual strength of carbon/epoxy flat plates. Using standardized test methods, unnotched plates are subjected to drop weight impact and fastener filled-hole plates are subjected to simulated lightning strike. Three different levels of damage are inflicted per test configuration, ranging from low-to-high threat levels. The resulting state of damage is measured non-destructively via ultrasonic C-scan and destructively via micrographic inspection. Results show that mechanical impact produces greater damage area than lightning strike. In both cases, damage is composed of a mix of extensive delaminations and matrix cracks and modest fiber breakage. After damage is inflicted, the plates are tested for CAI residual strength: results show that the strength degradation following mechanical impact is higher than lightning strike and the variation among specimens tested is smaller. Though a complex experimental setup, the energy dissipated in the lightning strike event is measured and compared to the energy dissipated in the mechanical impact event. Results show that the energy dissipated in a specimen during the lightning strike is much greater than the strain energy introduced by mechanical impact, and hence a comparison based on energy is not recommended. However, based on the relative threat levels associated with the impact and the lightning strike events, the comparison yields insightful observations on both damage resistance and tolerance behavior of the composite plates.

Acknowledgments

The authors would like to acknowledge the fundamental contributions of their colleagues Art Blair, Robert Gordon, and Tom Mattick and undergraduate research assistants Ben Renneberg, Andy Le, and Amy Nibert. They would also like to thank Robert Steinle, Diane Heidlebaugh, and Art Day (The Boeing Company) for their technical support and expert advice. The material for this study was supplied by Leslie Cooke of Toray Composites of America.

References

[1] Miller, A., "State of the Art Applications of Composites: The 787 Dreamliner," *22nd Annual Technical Conference of the American Society for Composites*, DEStech Publications, Inc., Lancaster, PA, Sept. 2007.

[2] Rupke, E., "Lightning Direct Effects Handbook," Lightning Technologies, Inc., Rept. AGATE-WP3.1-031027-043, Pittsfield, MA, 1 March 2002.

[3] Fisher, F. A., and Plumer, J. A., "Aircraft Lightning Protection Handbook," Lightning Technologies, Inc., Rept. FAA/CT-89/22, Sept. 1989.

[4] Feraboli, P., "Some Recommendations for the Characterization of the Impact Performance of Composite Panels by Means of Drop Tower Impact Testing," *Journal of Aircraft*, Vol. 43, No. 6, 2006, pp. 1710–1718.
doi:10.2514/1.19251

[5] Feraboli, P., and Kedward, K. T., "Enhanced Evaluation of the Low Velocity Impact Response of Composite Plates," *AIAA Journal*, Vol. 42, No. 10, 2004, pp. 2143–2152.
doi:10.2514/1.4534

[6] Kan, H. P., "Enhanced Reliability Prediction Methodology for Impact Damaged Composite Structures," U.S. Dept. of Transportation, Rept. DOT/FAA/AR-97/79, Oct. 1998.

[7] Heidlebaugh, D., Avery, W., and Uhrich, S., "Effect of Lightning Currents on Structural Performance of Composite Materials," *International Conference on Lightning and Static Electricity*, SAE International Paper 2001-01-2885, Seattle, WA, Sept. 2001.

[8] Feraboli, P., and Miller, M., "Damage Resistance and Tolerance of Carbon/Epoxy Composite Coupons Subjected to Simulated Lightning Strike," *Composites, Part A: Applied Science and Manufacturing*, Vol. 40, Nos. 6–7, 2009, pp. 954–967.

[9] "Certification of Transport Airplane Structure," U.S. Dept. of Transportation and Federal Aviation Administration, Advisory Circular AC 25-21, Sept. 1999, pp. 657.

[10] "Aircraft Lightning Zoning," SAE International, Rept. SAE ARP 5414, Warrendale, PA, 1999.

[11] "Aircraft Lightning Environment and Related Test Waveforms," SAE International, Rept. SAE ARP 5412, Warrendale, PA, 1999.

[12] "Damage Resistance, Durability, and Damage Tolerance," U.S. Dept. of Defense MIL-HDBK-17, Vol. 3, 2002, Rev. F, Chap. 7.

[13] Mitrovic, M., Hahn, H. T., Carman, G. P., and Shyprykevich, P., "The Effect of Loading Parameters on Fatigue of Composite Laminates," *Composites Science and Technology*, Vol. 59, No. 14, 1999, pp. 2059–2078.
doi:10.1016/S0266-3538(99)00061-5

[14] "Standard Test Method for Measuring the Damage Resistance of a Fiber-Reinforced Polymer Matrix Composite to a Drop-Weight Impact Event," *Book of Standards*, Vol. 15.03, ASTM International, Std. ASTM D7136, West Conshohocken, PA, 2009.

[15] "Standard Test Method for Measuring the Damage Resistance of a Fiber-Reinforced Polymer-Matrix Composite to a Concentrated Quasi-Static Indentation Force," *Book of Standards*, Vol. 15.03, ASTM International, Std. ASTM D6264, West Conshohocken, PA, 2009.

[16] "Standard Test Method for Compressive Residual Strength Properties of Damaged Polymer Matrix Composite Plates," *Book of Standards*, Vol. 15.03, ASTM International, Std. ASTM D7137, West Conshohocken, PA, 2009.

[17] "Standard Test Method for Open-Hole Compressive Strength of Polymer Matrix Composite Laminates," *Book of Standards*, Vol. 15.03, ASTM International, Std. ASTM D6484, West Conshohocken, PA, 2008.